Available online at www.sciencedirect.com
SCIENCE DIRECT®
Chemical Physics Letters 412 (2005) 399–405
CHEMICAL PHYSICS LETTERS
www.elsevier.com/locate/cplett

Extinction and orientational dependence of electron diffraction from single-walled carbon nanotubes

Zejian Liu [a], Lu-Chang Qin [a,b,*]

[a] Department of Physics and Astronomy, University of North Carolina at Chapel Hill, Campus Box 3255, Chapel Hill, NC 27599-3255, USA
[b] Curriculum in Applied and Materials Sciences, University of North Carolina at Chapel Hill, Chapel Hill, NC 27599-3255, USA

Received 5 May 2005; in final form 27 June 2005
Available online 1 August 2005

Abstract

The extinction and orientational dependence of electron diffraction from single-walled carbon nanotubes have been observed experimentally and investigated in detail theoretically using both algebraic analysis and numerical simulations. Electron diffraction from only achiral carbon nanotubes of zigzag or armchair structure shows observable orientational dependence and extinction of certain layer lines in experiment due to the interference of two primary Bessel functions of the same order that contribute to the scattering intensities on these layer lines.

1. Introduction

Carbon nanotubes possess many novel properties due to their unique structure. A single-walled carbon nanotube can be formed by wrapping up seamlessly a two-dimensional graphene along a chosen tubule axis [1,2]. The atomic structure of a single-walled carbon nanotube can be conveniently described by the perimeter vector $\vec{A} = u\vec{a}_1 + v\vec{a}_2$, or simply by the chiral indices (u, v), where $\vec{a}_1$ and $\vec{a}_2$ are the basis vectors defined on the graphene lattice with an inter-angle of 60° and lattice constant $a_1 = a_2 = a_0 = 0.2461$ nm. The diameter d and helicity α of the nanotube can then be expressed as $d = a_0\sqrt{u^2 + v^2 + uv}/\pi$ and $\alpha = \tan^{-1}[\sqrt{3}v/(2u + v)]$, respectively. Depending on the chiral indices, a carbon nanotube can be either metallic or semiconducting [3–6], which is of great importance in the envisaged nanoelectronics applications of this material.

Transmission electron microscopy (TEM) has played an essential role in characterizing the atomic structure of carbon nanotubes since their discovery [7]. Although the diameter of carbon nanotubes can be measured directly from the TEM images, the helicity usually has to be derived from the electron diffraction patterns [8–16]. Nanobeam electron diffraction, often performed in a transmission electron microscope equipped with a field emission gun, has been used in many applications recently to determine the atomic structure (both diameter and helicity) of carbon nanotubes. The small electron probe (normally on the order of 10 nm) can analyze an individual single-walled carbon nanotube with high accuracy. On the other hand, due to the tubular curvature of carbon nanotubes, the otherwise sharp Bragg reflections from the graphene structure are elongated perpendicular to the tubule axis, which can be described by Bessel functions of various orders as determined by the selection rule [17]. It has been shown that, for a chiral carbon nanotube of indices (u, v), the scattering intensity on each of the three principal layer lines is dominated by a single Bessel function $J_n(\pi dR)$ of an order n related to the chiral indices, i.e., $n_1 = v$, $n_2 = u$, and $n_3 = u + v$, and $I_{l1} \propto |J_v(\pi dR)|^2$, $I_{l2} \propto |J_u(\pi dR)|^2$, and $I_{l3} \propto |J_{u+v}(\pi dR)|^2$, respectively [15]. The atomic

* Corresponding author. Fax: +1 919 962 0480.
E-mail address: lcqin@physics.unc.edu (L.-C. Qin).

0009-2614/$ - see front matter © 2005 Elsevier B.V. All rights reserved.
doi:10.1016/j.cplett.2005.06.126

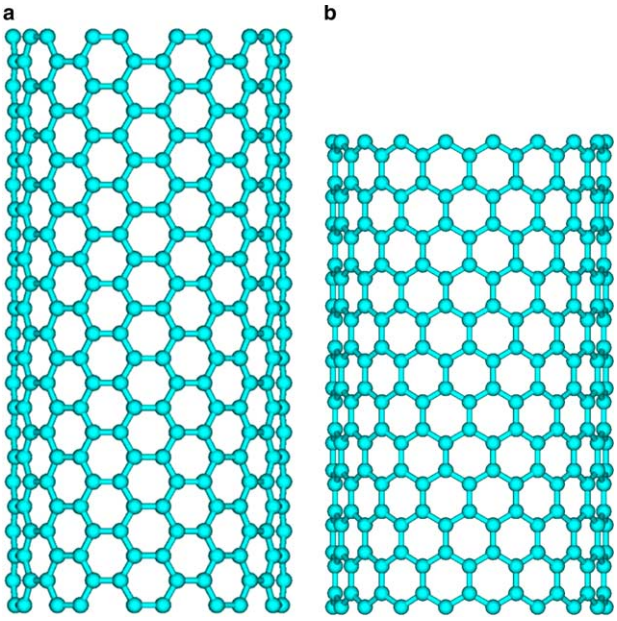

Fig. 1. Schematic of achiral carbon nanotubes: (a) armchair nanotube of chiral indices (10, 10); (b) zigzag nanotube of chiral indices (18, 0).

structure of every individual single-walled carbon nanotube can be determined unambiguously by applying this technique [16].

There have been several studies reported on the symmetry properties of electron diffraction from carbon nanotubes [18–22]. When the nanotube has a chiral structure, the electron scattering intensity as seen in an electron diffraction pattern is not sensitive to the orientation of the nanotube with respect to the incident electron beam [20]. However, when the nanotube has an achiral structure, i.e., either the zigzag or the armchair structure, whose chiral indices are $(u, 0)$ and (u, u), respectively, as schematically illustrated in Fig. 1, the electron diffraction intensity will become more sensitive on the orientation of the nanotube. A simple geometrical argument illustrates this effect clearly when the axial periodicity of the nanotube is halved at certain specific orientations [19].

In this Letter, we present a detailed analysis of the orientational dependence of electron diffraction patterns of single-walled carbon nanotubes illustrated by both experimental observations and numerical simulations. A general formula has also been derived to explain the orientational dependence for both the zigzag and the armchair nanotubes.

2. Experimental observation

Fig. 2a shows the TEM image of a single-walled carbon nanotube of zigzag structure and Fig. 2b is a nanobeam electron diffraction pattern of this nanotube, taken with a JEM 2010F TEM equipped with a field-emission

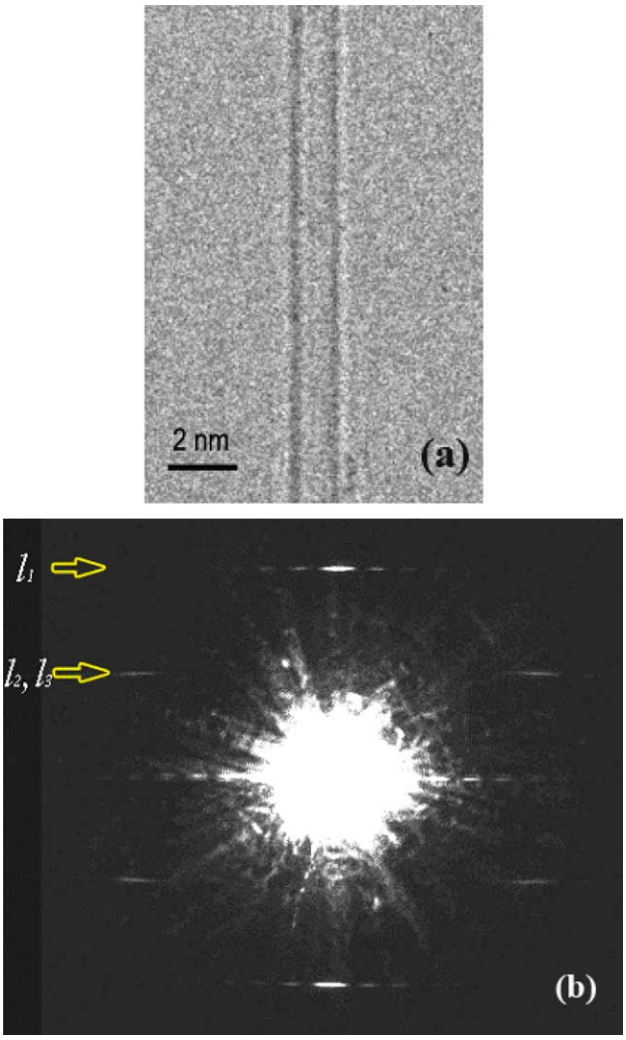

Fig. 2. (a) Electron microscope image of a single-walled carbon nanotube of diameter 1.3 nm. (b) Typical electron diffraction pattern of the nanotube. The diffraction patterns consist of layer lines in which the six strongest reflections due to the graphene structure are discernible. The intensities are elongated perpendicular to the tubule axis due to its finite radial dimensions.

gun operated at 80 kV in order to minimize the knock-on radiation damage to the nanotube. The incident electron beam is perpendicular to the tubule axis. The approximate diameter of the carbon nanotube can be measured directly from the TEM image, which is about 1.3 nm. Fig. 2b is a typical electron diffraction pattern of zigzag nanotube, where the principal layer lines l_2 and l_3 overlap and the six fundamental reflections due to the graphene structure show up clearly with significant intensities. Using the established procedure [15], the chiral indices of this nanotube are determined to be (16, 0), which is a semiconducting nanotube having diameter $d = 1.253$ nm.

Fig. 3a shows the TEM image of another zigzag nanotube of diameter 1.58 nm. The electron diffraction pattern of this nanotube is given in Fig. 3b from which

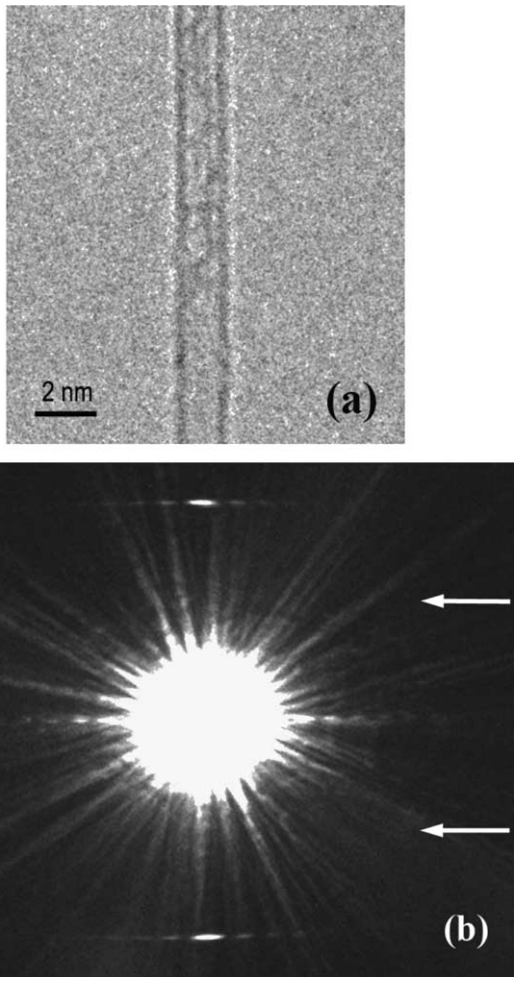

Fig. 3. (a) TEM image of a zigzag nanotube of diameter 1.58 nm. (b) Electron diffraction pattern of the nanotube of chiral indices (20, 0) where the extinction of the odd-layer lines ($l = \pm 1, \pm 3$) is shown, indicated by the arrows.

the chiral indices have been determined to be (20, 0). A salient feature of the electron diffraction pattern is the extinction of the first layer lines, one above and the other below the equatorial layer line as indicated by the arrows, whereas the second layer lines show significant scattering intensities in the electron diffraction pattern as in Fig. 2b.

3. Theoretical considerations

The electron scattering amplitude from a carbon nanotube of diameter d can be expressed analytically by [17]

$$F(R,\Phi,l) = \sum_n \exp[\mathrm{i}n(\Phi+\pi/2)]J_n(\pi\,\mathrm{d}R)\sum_j f \times \exp[\mathrm{i}(-n\phi_j + 2\pi l z_j/c)], \quad (1)$$

where f is the atomic scattering amplitude of carbon for electrons, c is the periodicity of the nanotube in the axial direction, $J_n(\pi\,\mathrm{d}R)$ is the Bessel function of order n, (R,Φ,l) are the cylindrical coordinates in the reciprocal space, and $(d/2,\phi_j,z_j)$ are the cylindrical coordinates of carbon atoms in the real space. In terms of the chiral indices (u, v), the selection rule that determines the orders of the dominating Bessel functions is

$$l = [(u+2v)n + 2(u^2+v^2+uv)m]/(uM), \quad (2)$$

where M is the maximum common divisor of $u+2v$ and $2u+v$, and m is an arbitrary integer that satisfies Eq. (2). Inserting the atomic positions of carbon atoms in a nanotube into Eq. (1), the scattering amplitude becomes [21]

$$F_{uv}(R,\Phi,l) = \sum_{n,m} f\chi_{uv}(n,m)\gamma_{uv}(n,m)\exp[\mathrm{i}n(\Phi+\pi/2)] \times J_n(\pi\,\mathrm{d}R), \quad (3a)$$

where

$$\chi_{uv}(n,m) = 1 + \exp[2\pi\mathrm{i}(n+(2u+v)m)/3u] \quad (3b)$$

and

$$\gamma_{uv}(n,m) = \begin{cases} u, & (n+mv)/u = \text{integer} \\ 0, & \text{otherwise.} \end{cases} \quad (3c)$$

For the nanotubes of zigzag structure, i.e., $(u,v) = (u, 0)$, the layer line selection rule equation (2) becomes $l = n/u + 2m$ and the orientational dependence of the scattering amplitude can be further reduced to

$$F_{u,0}(R,\Phi,l=\text{even}) = (\mathrm{i}2uf)\sum_{s=0}^{+\infty}\left[1+\exp\left(\mathrm{i}\frac{2\pi l}{3}\right)\right]J_{2su}(\pi\,\mathrm{d}R) \times \cos\left[2su\left(\Phi+\frac{\pi}{2}\right)\right]; \quad (4a)$$

and

$$F_{u,0}(R,\Phi,l=\text{odd}) = (\mathrm{i}2uf)\sum_{s=0}^{+\infty}\left[1+\exp\left(\mathrm{i}\frac{2\pi l}{3}\right)\right]J_{(2s+1)u}(\pi\,\mathrm{d}R) \times \sin\left[(2s+1)u\left(\Phi+\frac{\pi}{2}\right)\right]. \quad (4b)$$

The summation over s is for all non-negative integers. Since only the Bessel functions of the lowest orders contribute significantly to the total intensities on a layer line [21], the significant terms in Eq. (4) are the Bessel functions of the lowest orders and we can express the diffraction intensities as

$$I_{u,0}(R,\Phi,l=\text{even}) \approx 16u^2f^2|J_0(\pi\,\mathrm{d}R)|^2\left\{1+\frac{2J_{2u}(\pi\,\mathrm{d}R)}{J_0(\pi\,\mathrm{d}R)} \times \cos\left[2u\left(\Phi+\frac{\pi}{2}\right)\right]\right\}\cos^2\left(\frac{\pi l}{3}\right), \quad (5a)$$

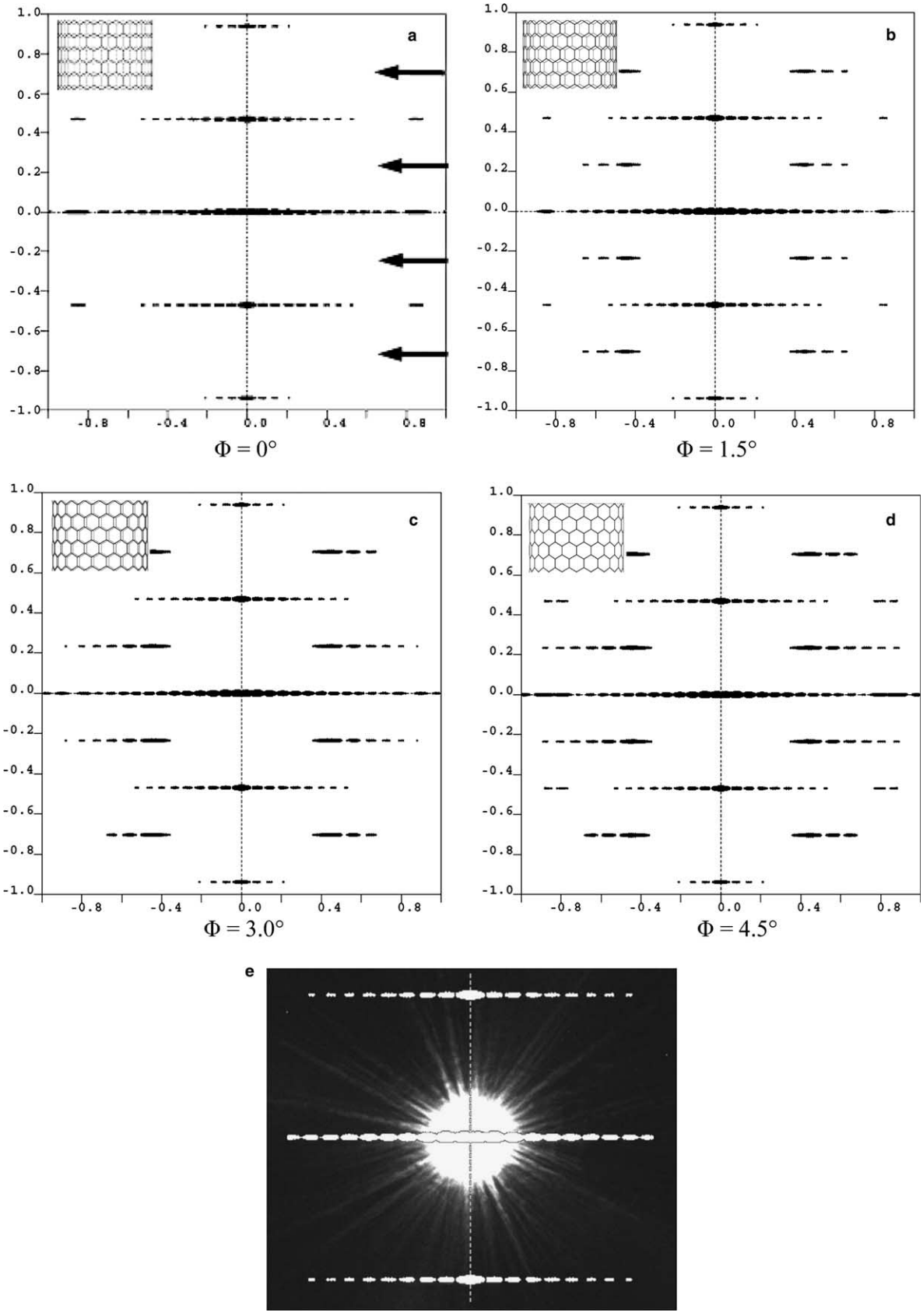

Fig. 4. Calculated intensity distribution of electron diffraction as a function of azimuthal orientation Φ of nanotube (20, 0). (a) $\Phi = 0°$, where extinction occurs as indicated by the disappearance of the first layer line indicated by the arrows. (b) $\Phi = 1.5°$. (c) $\Phi = 3.0°$. (d) $\Phi = 4.5°$. (e) Overlap of the experimental electron diffraction pattern (Fig. 2) and the calculated one (a).

and

$$I_{u,0}(R,\Phi,l=\text{odd}) \approx 16u^2f^2|J_u(\pi\,\mathrm{d}R)|^2\cos^2(\pi l/3)\sin^2[u(\Phi+\pi/2)]. \tag{5b}$$

The intensity distribution is modulated by both the dominating Bessel functions and the orientational variable Φ. For the layer lines of even indices (Eq. (5a)), the intensity dependence on the nanotube orientation is weak. However, for the layer lines of odd indices (Eq. (5b)), the layer line intensity distribution is modulated by $\sin^2[u(\Phi+\pi/2)]$, which gives rise to much stronger dependence on the orientational parameter Φ (azimuthal angle) with a periodicity of π/u, though the angular structural periodicity is $2\pi/u$. Because of this azimuthal modulation, extinction reflections occur at the following orientations:

$$\Phi_{\text{ext}} = \begin{cases} N\pi/u & (u=\text{even}), \\ (2N+1)\pi/(2u) & (u=\text{odd}), \end{cases} \quad N=0,1,2,\ldots,(2u-1). \tag{6}$$

There are total $2u$ orientations in which extinction takes place with an interval of π/u.

For nanotubes of armchair structure, i.e., $(u, v) = (u, u)$, the layer line selection rule is the same as that for zigzag nanotubes, $l = n/u + 2m$, and the orientational dependence of the electron scattering intensities can be obtained similarly

$$I_{u,u}(R,\Phi,l=\text{even}) \approx 16u^2f^2J_0^2(\pi\mathrm{d}R)\left\{1+\frac{J_{2u}(\pi\,\mathrm{d}R)}{J_0(\pi\,\mathrm{d}R)}\cos\left[2u\left(\Phi+\frac{\pi}{2}\right)-\frac{\pi}{3}\right]\right\} \tag{7a}$$

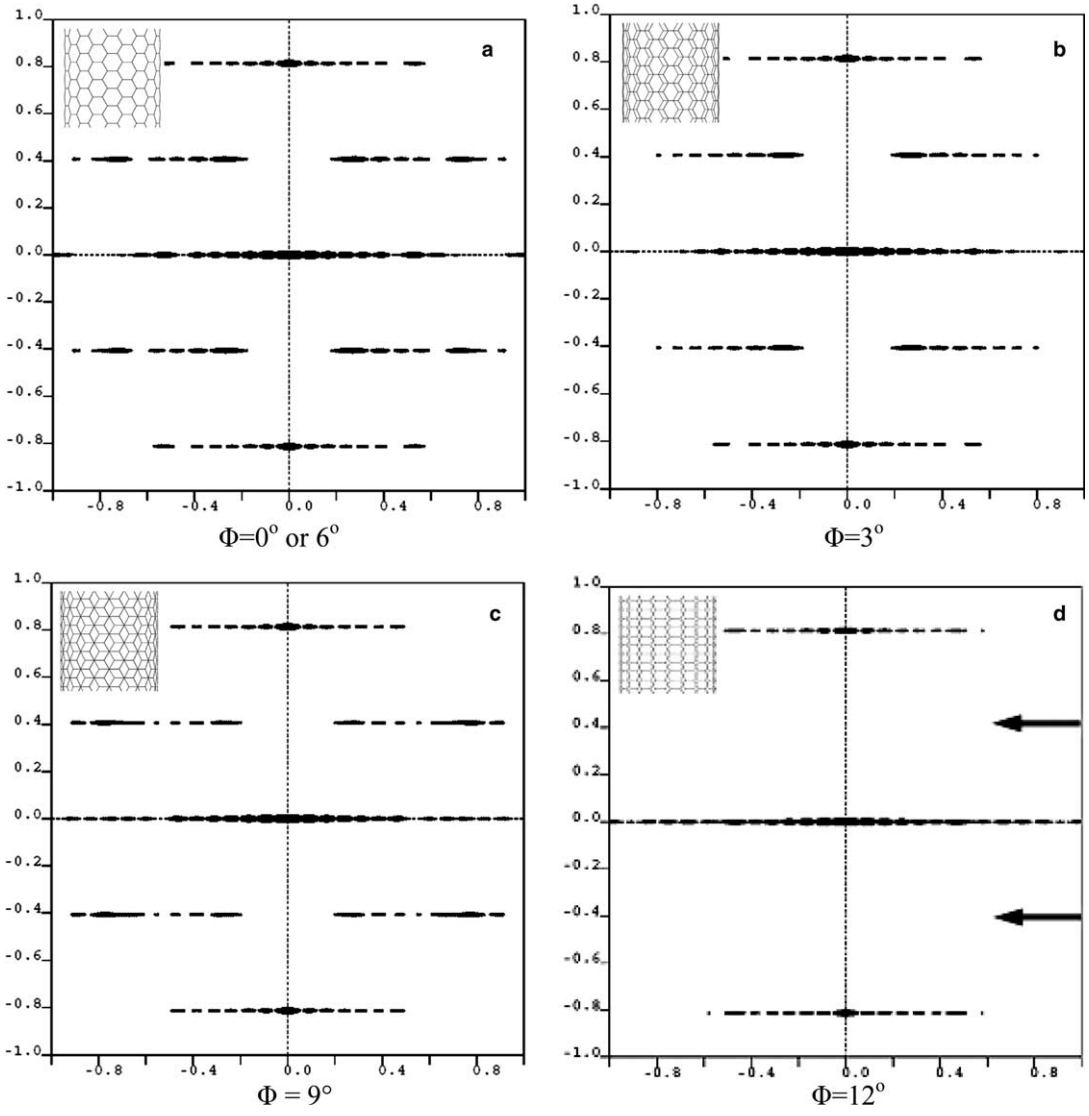

Fig. 5. Calculated electron diffraction patterns of armchair carbon nanotube (10, 10) as a function of the nanotube orientation specified by the angular coordinate Φ. (a) $\Phi = 0°$ or 6°. (b) $\Phi = 3°$. (c) $\Phi = 9°$. (d) $\Phi = 12°$ where extinction occurs. The extinction layer lines ($l = \pm 1$) are indicated by arrows.

and

$$I_{u,u}(R, \Phi, l = \text{odd}) \approx 4u^2 f^2 J_u^2(\pi\, \mathrm{d}R)\sin^2[u(\Phi + \pi/2) + \pi/3]. \quad (7b)$$

Like the case for the zigzag nanotubes, the orientational dependence in the even layer lines are secondary (Eq. (7a)) and a total extinction occurs on the odd-layer lines when

$$\Phi_{\text{ext}} = \begin{cases} (3N+2)\pi/(3u) & (u = \text{even}), \\ (6N+1)\pi/(6u) & (u = \text{odd}), \end{cases} \quad N = 0, 1, 2, \ldots, (2u-1). \quad (8)$$

There are also $2u$ orientations in which extinction occurs with an interval of π/u.

The orientational periodicity can assist in the determination of the chiral indices of the zigzag nanotube $(u, 0)$ and the armchair nanotube (u, u) when the orientational dependence is measured in high precision.

4. Results and discussion

For the zigzag single-walled carbon nanotube (20, 0), its angular structural periodicity is 18°, and the intensity distribution is periodic in repetition of 9°. The total number of extinction orientations is 40 across the cylindrical circumference with an interval of $\Delta\Phi = 2\pi/40 = 9°$. Figs. 4a–d show the calculated electron scattering intensities from the zigzag nanotube (20, 0) at azimuthal orientations (projected structure of the zigzag nanotube is also given in each figure) $\Phi = 0°$, 1.5°, 3.0° and 4.5°. A total extinction of the odd-layer lines occurs at $\Phi = 0°$ (Fig. 4a). The calculations and the experimental observation are in excellent agreement as indicated in Fig. 4e where the theoretical data (Fig. 4a) are plotted on the experimental electron diffraction data (Fig. 3).

Fig. 5 shows the calculated electron diffraction patterns of an armchair nanotube (10, 10) at orientations $\Phi = 0°$, 3°, 9° and 12°. For the armchair nanotube (10, 10), the diffraction intensity distribution at $\Phi = 6°$ is the same as $\Phi = 0°$. The interval between neighboring extinction orientations is 18°. Extinction on the odd-layer lines occurs at $\Phi = 12°$ (Fig. 5d).

The occurrence of extinction is due to the fact that at certain specific orientations, the periodicity of the projected structure of the achiral nanotube in the axial direction is halved. The projected structure with a halved periodicity at these specific orientations, as illustrated in Figs. 4a and 5d, results in the doubling of the layer line spacings in the reciprocal space [19].

Understanding of the orientational dependence is very important for a comprehensive understanding of the electron diffraction patterns from carbon nanotubes for structure analysis. Electron diffraction patterns can be obtained either upon normal incidence or upon inclined incidence of the electron beam. Since the achiral carbon nanotubes show significant orientational dependence, upon tilting the 2mm symmetry of the electron diffraction patterns from an achiral carbon nanotube may break down [20], although the inversion symmetry is always preserved. In comparison, electron diffraction patterns of chiral carbon nanotubes always show 2mm symmetry in experiment [21]. In addition, the orientational dependence of electron diffraction from multi-walled carbon nanotubes is also very useful for studying the relative handedness of the composing shells [22,23].

5. Conclusions

The scattering intensities in electron diffraction patterns of achiral (zigzag or armchair) single-walled carbon nanotubes show strong orientational dependence as a result of the interference of two Bessel functions of the same order on the odd-indexed layer lines. Extinction of these layer lines occurs at specific orientations of the achiral carbon nanotube relative to the incident electron beam. The periodicity of orientational dependence and extinction of the layer lines in the electron diffraction patterns is related to the chiral indices of zigzag nanotube $(u, 0)$ and armchair nanotube (u, u) by π/u.

References

[1] S. Iijima, T. Ichihashi, Nature (London) 363 (1993) 603.
[2] D.S. Bethune, C.H. Kiang, M.S. Devries, G. Gorman, R. Savoy, J. Vazquez, R. Beyers, Nature (London) 363 (1993) 605.
[3] R. Saito, M. Fujita, G. Dresselhaus, M.S. Dresselhaus, Appl. Phys. Lett. 60 (1992) 2204.
[4] N. Hamada, S. Sawada, A. Oshiyama, Phys. Rev. Lett. 68 (1992) 1579.
[5] J.W.G. Wildoer, L.C. Venema, A.G. Rinzler, R.E. Smalley, C. Dekker, Nature (London) 391 (1998) 59.
[6] T.W. Odom, J.L. Huang, P. Kim, C. Lieber, Nature (London) 391 (1998) 62.
[7] S. Iijima, Nature (London) 354 (1991) 56.
[8] L.-C. Qin, T. Ichihashi, S. Iijima, Ultramicroscopy 67 (1997) 181.
[9] J.M. Cowley, P. Nikolaev, A. Thess, R.E. Smalley, Chem. Phys. Lett. 265 (1997) 379.
[10] L.-C. Qin, S. Iijima, H. Kataura, Y. Maniwa, S. Suzuki, Y. Achiba, Chem. Phys. Lett. 268 (1997) 101.
[11] L.-C. Qin, Chem. Phys. Lett. 297 (1998) 23.
[12] M. Kociak, K. Suenaga, K. Hirahara, Y. Saito, T. Nakahira, S. Iijima, Phys. Rev. Lett. 89 (2002) 155501.
[13] M. Gao, J.M. Zuo, R.D. Twesten, I. Petrov, L.A. Nagahara, R. Zhang, Appl. Phys. Lett. 82 (2003) 2703.
[14] J.M. Zuo, I. Vartanyants, M. Gao, R. Zhang, L.A. Nagahara, Science 300 (2003) 1419.
[15] Z.J. Liu, L.-C. Qin, Chem. Phys. Lett. 408 (2005) 75.
[16] Z.J. Liu, Q. Zhang, L.-C. Qin, Phys. Rev. B 71 (2005) 245413.

[17] L.-C. Qin, J. Mater. Res. 9 (1994) 2450.
[18] X.F. Zhang, X.B. Zhang, G. Van Tendeloo, S. Amelinckx, M. Op de Beeck, J. Van Landuyt, J. Cryst. Growth 130 (1993) 368.
[19] S. Amelinckx, A.A. Lucas, P. Lambin, Rep. Prog. Phys. 62 (1999) 1471.
[20] K. Hirahara, S. Bandow, H. Kataura, M. Kociak, S. Iijima, Phys. Rev. B 70 (2004) 205422.
[21] Z.J. Liu, L.-C. Qin, Chem. Phys. Lett. 400 (2004) 430.
[22] Z.J. Liu, L.-C. Qin, Chem. Phys. Lett. 402 (2005) 202.
[23] Z.J. Liu, L.-C. Qin, Chem. Phys. Lett. 411 (2005) 291.